Further evidence for ultrahigh-energy cosmic ray acceleration in starburst-driven superwinds

Luis Alfredo Anchordoqui

Department of Physics and Astronomy, Lehman College, City University of New York, New York, New York 10468, USA;
Department of Physics, Graduate Center, City University of New York, New York, New York 10016, USA; and Department of Astrophysics, American Museum of Natural History, New York, New York 10024, USA

(Received 11 December 2022; accepted 4 April 2023; published 19 April 2023)

Very recently, the Pierre Auger and Telescope Array collaborations reported strong evidence for a correlation between the highest energy cosmic rays and nearby starburst galaxies, with a global significance post-trial of 4.7σ. It is well-known that the collective effect of supernovae and winds from massive stars in the central region of these galaxies drives a galactic-scale superwind that can shock heat and accelerate ambient interstellar or circumgalactic gas. In previous work we showed that, for reasonable source parameters, starburst-driven superwinds can be the carriers of ultrahigh-energy cosmic ray acceleration. In this paper we assess the extent to which one can approach the archaeological "inverse" problem of deciphering properties of superwind evolution from present-day IR emission of their host galaxies. We show that the Outer Limits galaxy NGC 891 could provide "smoking-gun evidence" for the starburst-driven superwind model of ultrahigh-energy cosmic rays.

DOI: 10.1103/PhysRevD.107.083024

I. INTRODUCTION

It is difficult to overstate the scientific importance of understanding the origin of the highest-energy cosmic rays. Ultrahigh-energy cosmic rays (UHECRs) have been observed since the early 1960's [1] and a plethora of models have been proposed to explain their origin, including acceleration (bottom-up) processes in power astrophysical environments and (top-down) decay of super-heavy (GUT scale) particles [2].

In the late 1990's we proposed a model predicting that UHECR nuclei could be accelerated in the large-scale terminal shock of the superwinds that flow from the central region of starburst galaxies [3]. A few years later we also predicted that the highest energy cosmic ray nuclei will generate 20 to 30 degrees hot-spots around the starbursts, because of their magnetic deflection in the Galactic magnetic field [4].

Over the last decade, mounting evidence has been accumulating suggesting that the UHECR composition becomes dominated by nuclei at the high-energy end of the spectrum [5–10]. Concurrently, the Pierre Auger Collaboration has provided a compelling indication for a possible correlation between the arrival directions of cosmic rays with energy $E \gtrsim 10^{10.6}$ GeV and a model based on a catalog of bright starburst galaxies [11,12]. The post-trial chance probability in an isotropic cosmic ray sky gives a Gaussian significance of 4.0σ. When data from the Telescope Array are included in the statistical analysis the correlation with starburst galaxies is stronger than the Auger-only result, with a post-trial significance of 4.7σ [13]. In the best-fit model, $(12.1 \pm 4.5)\%$ of the UHECR flux originates from the starbursts and undergoes angular diffusion on a von Mises-Fisher scale $\psi \sim 15.1^{+4.6^\circ}_{-3.0}$.[1]

Together these observations lead to two critical questions:

(i) What imprints may the evolution of starburst-driven superwinds leave in present-day observables?
(ii) To what extent can we decipher this archaeological record, exploiting information about the present-day Universe in order to learn about or constrain the possible acceleration of UHECR nuclei in starburst-driven superwinds?

These are certainly very broad questions, and in this paper we attempt to take a first step towards answering these questions.

Before proceeding, we pause to note that median deflections of particles in the Galactic magnetic field are estimated to be

$$\theta_G \sim 3^\circ Z \left(\frac{E}{10^{11}\ \text{GeV}} \right), \tag{1}$$

[1]It is important to note that a likelihood analysis considering the biases induced by the coherent deflection in the Galactic magnetic field gives best-fit parameters which are consistent within 95% C.L. with those obtained adopting angular diffusion in the isotropic-scattering approximation [14].

where Z is the charge of the UHECR in units of the proton charge [15]. Thus, the requirement $\theta_G \lesssim \psi$ implies that UHECRs contributing to the starburst anisotropy signal should have $Z \lesssim 10$ and $E/Z \sim 10^{10}$ GeV.

II. STARBURST ARCHEOLOGY

Starburst-driven superwinds are complex, multi-phase phenomena primarily powered by the momentum and energy injected by massive stars in the form of supernova (SN) explosions, stellar winds, and radiation [16]. According to the book, these superwinds are ubiquitous in galaxies where the star-formation rate per unit area exceeds $10^{-1} M_\odot\ \mathrm{yr}^{-1}\,\mathrm{kpc}^{-2}$. This type of starbursting object, nicknamed far-IR galaxy (FIRG), can be characterized by *(i)* an IR luminosity, $L_{\rm IR} \gtrsim 10^{44}\ \mathrm{erg\,s}^{-1}$, which is large relative to its optical luminosity $L_{\rm IR} \gg L_{\rm OPT}$, and *(ii)* a "warm" IR spectrum (flux density at 60 μm > 50% the flux density at 100 μm).

The deposition of mechanical energy by supernovae and stellar winds results in a bubble filled with hot ($T \lesssim 10^8$ K) gas that is unbound by the gravitational potential because its temperature is greater than the local escape temperature. The overpressured bubble expands adiabatically, becomes supersonic at the edge of the starburst region, and eventually blows out of the disk into the halo forming a strong shock front on the contact surface with the cold gas in the halo.

Two distinct mechanisms have been proposed to explain the starburst anisotropy signal:

(i) UHECRs can be accelerated by bouncing back and forth across the superwind's terminal shock (hereafter ARC model) [3].

(ii) UHECR acceleration can occur in the disproportionally frequent extreme explosions that take place in the starburst nucleus due to the high star-formation activity [17]; e.g., low-luminosity gamma-ray bursts (llGRBs) [18].

A point worth noting at this juncture is that one would expect llGRB explosions to stochastically sample the locations of cosmic-star formation throughout the volume of the Universe in which they can be observed. Then the probability for a given type of galaxy to host a llGRB during some period of time would be proportional to its star-formation rate. Starburst galaxies represent about 1% of the fraction of galaxies containing star-forming galaxies [19], and the probability of SN explosions is about one to two orders of magnitude larger in starbursts than in normal galaxies, e.g., the SN rate for M82 is about 0.2–0.3 yr^{-1} [20] whereas for the Milky Way is $\sim 3.5 \pm 1.5\ \mathrm{century}^{-1}$ [21]. Note that these two effects tend to compensate each other, and so a straightforward calculation shows that UHECRs accelerated in llGRBs will have a stronger correlation with the nearby matter distribution than with starbursts [22].

Indeed, given the ubiquity of llGRB explosions we can ask ourselves why the correlation of UHECRs with starburst galaxies would be explained by the presence of this *common* phenomenon. Rather there must be some other inherently unique feature of starburst galaxies to account for this correlation. With this in mind, herein we focus on the ARC model [3]. In previous work [23,24], we investigated the constraints imposed by the starburst anisotropy signal on the ARC model and we readjusted free parameters to remain consistent with the most recent astrophysical observations. We now investigate the minimum power requirement for UHECR acceleration at shocks.

The cosmic ray maximum energy for any multiplicative acceleration process is given by the Hillas criterion, which yields $E_{\rm max} \sim ZeuBR$, where R is the size and B the magnetic field strength of the acceleration region, and u is the speed of the scattering centers (i.e., the shock velocity) [25]. Now, the magnetic field B carries with it an energy density $B^2/(2\mu_0)$, and the outflowing plasma carries with it an energy flux $\sim uR^2B^2/(2\mu_0)$, where μ_0 is the permeability of free space. This sets a constraint on the maximum magnetic power delivered through the shock [26]. Following [27], we combine the Hillas criterion with the constraint of the magnetic energy flux to arrive at the minimum power needed to accelerate a nucleus to a given rigidity $\mathcal{R}$,

$$\mathcal{P}_{\rm min} = \frac{\mathcal{R}^2}{2\mu_0 u} \sim 10^{44}\,\mathrm{erg\,s}^{-1} \left(\frac{u}{0.01\,c}\right)^{-1} \left(\frac{\mathcal{R}}{10^{10}\,\mathrm{GV}}\right)^2. \tag{2}$$

This steady-state argument provides a conservative upper limit for the required minimum power in the superwind. Note that the minimum power requirement can be relaxed if, e.g., the energy carried by the out-flowing plasma needed to maintain a 100 μG magnetic field strength on a scale of 15 kpc [24] is supplied during periodic flaring intervals. Throughout we remain cautious and adopt (2) as our point of reference.

Next, in line with our stated plan, we adopt the functional form of the energy injection rate from stellar winds and supernovae estimated in [28] to determine the kinetic energy output of the starburst from measurements of the IR luminosity,

$$\mathcal{P}_{\rm today} \sim 4 \times 10^{43} L_{\rm IR,11}\ \mathrm{erg\,s}^{-1}, \tag{3}$$

where $L_{\rm IR,11}$ is the total IR luminosity (in units of $10^{11} L_\odot$), and where we have rescaled the normalization factor to accommodate a supernova rate in M82 of 0.3 yr^{-1} [29], rather than the 0.07 yr^{-1} used in the original calculation of [28]. The associated mass-loss rate to match the normalization $u \sim 0.01\,c$ is found to be

$$\dot{M} \sim 15 L_{\rm IR,11} M_\odot\ \mathrm{yr}^{-1}. \tag{4}$$

TABLE I. Infrared luminosities [30] and kinetic energy output.

Starburst galaxy	$\log_{10}(L_{\rm IR}/L_\odot)$	$\mathcal{P}_{\rm today}/(10^{43}\ {\rm erg\ s^{-1}})$
NGC 253	10.44	1
NGC 891	10.27	0.7
NGC 1068	11.27	7
NGC 3034 (a.k.a. M82)	10.77	2
NGC 4945	10.48	1
NGC 5236 (a.k.a. M83)	10.10	0.5
NGC 6946	10.16	0.6
IC 342	10.17	0.6

In Table I we list the present-day kinetic energy output of the nearby starbursts contributing to the anisotropy signal.

By comparing (2) with the results on Table I we see that for most of the starbursts the present-day power output falls short by about an order of magnitude to accommodate the required maximum rigidity to explain the anisotropy signal. However, we note that the estimate in (2) is subject to large systematic uncertainties; see Appendix A. Furthermore, the characteristic timescale for Fermi acceleration in nonrelativistic shocks is $\mathcal{O}(10^7\ {\rm yr})$ [31], and the superwind power given in Table I does not take into account any source evolution, but rather characterizes the current state of the outgoing plasma assuming that the star formation proceeded continuously at a constant rate.

The question is then; Could the superwind of the FIRGs listed in Table I be more powerful in an earlier stage? The answer to this question is, in principle, yes. with the rationale being that very powerful FIRGs have been observed in our cosmic backyard. For example, Arp 220 and NGC 6240 are the nearest and best-studied examples of very powerful FIRGs ($L_{\rm IR}\sim 10^{12}L_\odot$), while IRAS 00182–7112 is the most FIR-powerful galaxy yet discovered ($L_{\rm IR}$ nearly $10^{13}L_\odot$) [28]. We note, however, that there is no solid evidence indicating that these powerful FIRGs could represent an early stage of the starburst evolution. The star formation history of Arp 220 is multiplex: in the central kpc, a 10 Myr old starburst provides the majority of the IR luminosity [32]. This is comparable to the mean age of the active starburst in M82, but somewhat younger than the stellar activity powering the central regions of NGC 253, see Appendix A. What's more, data from supernova radio spectra of Arp 220 may be indicative of a very short, intense burst of star formation around 3 Myr ago [33], which could be the elephant in the room.

Now, the anisotropy correlation is observed to be spread over an angular region of size $\sim 20°$.[2] The spread originates in the scattering of UHECRs with magnetic fields as they propagate to the Earth. The scattering on magnetic fields also gives rise to a spread in the arrival times of UHECRs with respect to the IR emission. If all scattering takes place in the Milky Way the dispersion in the UHECR arrival times is roughly 10^3 yr [34]. This seems a very short period of time to accommodate an order of magnitude change in $\mathcal{P}$. However, since the number density of gas in the halo region is $10^{-3}\lesssim n_{{\rm g},h}/{\rm cm}^3\lesssim 10^{-2}$ [35–38] and the total pp cross section at $E\sim 10^{10}$ GeV is $\sigma_{pp}\sim 100$ mb, the characteristic timescale for pp collisions in the acceleration region is $1\lesssim\tau_{\rm int}^{pp}/{\rm Gyr}\lesssim 10$. For a nucleus of baryon number A scattering off a proton, an order of magnitude estimate of the total cross section can be obtained from the empirical scaling $\sigma_{Ap}\sim A^{2/3}\sigma_{pp}$ [39]. Thereby, for a medium mass nucleus (carbon, nitrogen, or oxygen), the characteristic timescale to scatter off the gas in the acceleration region is $0.1\lesssim\tau_{\rm int}^{Ap}/{\rm Gyr}\lesssim 1$. Moreover, the energy-loss rate of baryon scattering is comparable to that of nucleus photodisintegration in the background radiation fields of the acceleration region, see Appendix B. All in all, this implies that even considering the upper range for estimates of the gas density in the halo, UHECRs ARC accelerated by the starburst superwind could be storaged in the acceleration region without suffering catastrophic spallations.

At last, we adopt the venerable leaky-box approximation to outline a first order model that can describe the dynamics of the starburst emission process. In analogy with the *closed Galactic model* of [40], we start with the assumption that, in a first stage, during the ARC acceleration process all cosmic rays remain confined to the galaxy by a suitable large magnetic field, even at the highest energies. In a second stage, the confinement power of the magnetic field (correlated with $L_{\rm IR}$) gradually decreases and the UHECRs are trapped, but within reflecting boundaries surrounding the galaxy, such that at each encounter with the boundary, they have a time-dependent probability of escaping into the intergalactic space. This leakage of UHECRs is driven by diffusion with a time-dependent rigidity, but of course the larger the rigidity the less time spent in the confinement volume.

To develop some sense for the orders of magnitude involved, we recall that in each "scatter," the diffusion coefficient describes an independent angular deviation of particle trajectories whose magnitude depends on the Larmor radius $r_L=0.1Z^{-1}E_{10}B_{100}^{-1}$ kpc, where $E_{10^{10}}=E/10^{10}$ GeV and $B_{100}=B/100\ \mu$G [2].[3] That said, it is reasonable to assume that a medium mass nucleus with $E\lesssim 10^{10.7}$ GeV would remain trapped inside magnetic subdomains of size $\ell\sim 0.1$ kpc, attaining efficient

[2]The angular spread of a von Mises-Fisher distribution, the equivalent of a Gaussian on the sphere, corresponds to a top-hat scale $\Psi\sim 1.59\times\psi$.

[3]Our fiducial choice of B is supported by full-blown simulations, which accurately capture the hydrodynamic mixing and dynamical interactions between the hot and cold phases in the outflow [41]; for details, see [24].

diffusion when the wave number of the associated Alfvén wave is equal to the Larmor radius of the nucleus [42]. With a Kolmogorov form for the turbulent magnetic field power spectrum (with coherent directions on scales ℓ), this gives for a diffusion coefficient

$$D(E) \sim 5 \ell_{0.1}^{2/3} B_{100}^{-1/3} E_{10^{10}}^{1/3} \frac{\mathrm{kpc}^2}{\mathrm{Myr}}, \tag{5}$$

where $\ell_{0.1} = \ell/0.1$ kpc [43]. Neglecting a numerical constant of order one, the diffusion time to the "magnetic wall" is estimated to be $\tau_{\rm diff}(E) \sim H^2/D(E)$, where H is the height of the halo [44]. For $H \sim 15$ kpc [45], the diffusion time is in the ballpark, $\tau_{\rm diff}(E) \sim 50\ \mathrm{Myr}/E_{10^{10}}^{1/3}$. Note that a mean residence time in the confinement volume of $\tau_{\rm res} \sim 0.1$ Gyr, would require cosmic rays to bounce one ($E \sim 10^{10}$ GeV) or two ($E \sim 10^{10.7}$ GeV) times in the reflecting boundaries. Therefore, for the problem at hand, the ratio of the diffusion coefficient in the wall to that in the confinement volume must not be unreasonably high. This is in sharp contrast to the classical leaky box description of Galactic cosmic rays [46].

Needless to say, the *ad hoc* assumption that the residence time of UHECRs is compatible with a single value is a rudimentary order of magnitude approximation, because particles originated in the center reside longer that those populating the halo periphery. A precise description of the storage/trapping mechanism, with a time-dependent probability of escaping into the intergalactic space, requires a numerical simulation that is beyond the scope of this paper. Besides, one may object our choice of fiducial values for B and H, which could be considered somewhat off-center. Whichever point of view one may find more convincing, it seems most conservative at this point to depend on experiment (if possible) to resolve the issue. In the next section we examine a particular FIRG example that could provide a clear-cut experimental test of the ideas discussed above.

III. NGC 891: THE SMOKING GUN

The Outer Limits spiral galaxy NGC 891 lives in the Local Super Cluster, some 9.7 Mpc away.[4] The galaxy looks as the Milky Way would look like when viewed edge-on, and indeed the two galaxies are considered very similar in terms of luminosity and size [47]. However, HI observations reveal structures on various scales. High resolution images of its dusty disk show unusual filament patterns extending into the halo of the galaxy, away from its galactic disk. The overall kinematics of the gas in the halo is characterized by differential rotation lagging with respect to that of the disk. The lag, which is more pronounced at small radii, increases with height from the plane. There is evidence that a significant fraction of the halo is due to a galactic fountain [48].

The slope of the luminosity function is powerful indicator of the main features of the host galaxy. On the one hand, if the star formation rate in the galaxy is constant, then the luminosity function describing the sources can be accommodated by a single unbroken power-law model. On the other hand, if the galaxy is starbursting then new high-mass x-ray binaries would be formed, breaking the luminosity function slope. The break in the slope would decrease with time, and would be an indication of the time of previous bursts in the galaxy. The x-ray luminosity function of NGC 891 can be fitted by a single power law, but with a slope typical of starburst galaxies and flux density ratio (at 60 μm/100 μm) corresponding more to normal spirals than starbursts [49]. Altogether this indicates that NGC 891 is a starburst in a quiescent state.

NGC 891, located in equatorial coordinates at (right ascension, declination) = $(35.64°, 42.35°)$, is inside the ∼20° angular window where the Telescope Array Collaboration reported an excess of events over expectations from isotropy [50]. More precisely, the hotspot is centered at $(19°, 35°)$, and has a local significance of 4σ down to $E \sim 10^{10.1}$ GeV.[5] More data are certainly needed to ascertain whether the hot spot originates in NGC 891. Should this be the case, it is clear that UHECR acceleration must have occurred in the past, when the galaxy was starbursting.

Note that, in very good approximation, UHECRs are emitted instantaneously by llGRB and they cannot remain unscathed inside the starburst core. Indeed, the production of very- and ultrahigh energy neutrinos would be a clear indication that UHECRs are accelerated in the central region of the starburst [51,52]. In contrast, in the ARC model, the interaction of UHECRs with the gas and radiation fields in the halo is largely suppressed (for details, see Appendix C), and therefore the neutrino signal would be largely suppressed.

We stress once more that NGC 891 is a starburst in a quiescent state. Because of this, the production of UHECRs assuming typical starburst properties must have occurred in the past, when the starbursting nucleus was active. Now, since these cosmic rays cannot be storaged in the nucleus, but only in the halo, we can conclude that the confirmation of NGC 891 as an UHECR source would disfavor acceleration through powerful explosions in the starburst nucleus, while providing some support for ARC acceleration with time-dependent reflecting boundaries surrounding the galaxy.

IV. CONCLUSIONS

We have investigated whether starburst-driven superwinds satisfy the power requirements to accelerate

[4]NGC 891 appears in the end credits of the Outer Limits 1963 TV series.

[5]We used $E_{\rm Auger} = E_0 e^{\alpha} (E_{\rm TA}/E_0)^{\beta}$, with $E_0 = 10^{10}$ GeV, $\alpha = -0.159 \pm 0.012$ and $\beta = 0.945 \pm 0.016$ [13].

UHECRs. Since the acceleration timescale is $\mathcal{O}(10^7$ yr), this quest by necessity has been fundamentally archaeological: we seek to exploit present-day observations in the interest of learning about the past. We have shown that NGC 891 provides fossil evidence that UHECRs may have been ARC accelerated in the past and remained storaged in the acceleration region, where they diffused rather freely without suffering significant energy losses. When the confinement power of the magnetic field (correlated with $L_{\rm IR}$) in the storage region started to gradually decrease a fraction of the cosmic rays began to escape at a rate that has slowly increased over time.

ACKNOWLEDGMENTS

The research of L. A. A. is supported by the U.S. NSF Grant No. PHY-2112527.

APPENDIX A: SYSTEMIC UNCERTAINTIES

The estimate of the kinetic energy output for the starbursts is model dependent, and therefore subject to large systematic uncertainties. One source of uncertainty is the functional form relating $\mathcal{P}$ and $L_{\rm IR}$. A commonly-used, simplifying assumption when modeling the starburst histories is that the star formation proceeds continuously at a constant rate [53]. For a constant star formation rate (SFR), the Salpeter stellar initial mass function (IMF) [54] leads to ratios $\mathcal{P}_{\rm today}/L_{\rm IR,11}$ and $\dot{M}/L_{\rm IR,11}$ which are a factor of $\sim$3 smaller than the fiducial values given in (3) and (4) [55]. A factor of $\mathrm{SFR}_{[46]}/\mathrm{SFR}_{[45]} \sim 1.5$ comes from the adopted relation between SFR and $L_{\rm IR}$ derived in [56] assuming that the mass spectrum between 10 and $100M_\odot$ follows a power law with slope 2.35 [57]. IMFs which are considerably flatter than the Salpeter IMF lead to higher values of $\mathcal{P}_{\rm today}$ [58]. However, the point we want to make herein is not only that the uncertainty in the empirically determination of the proportionality constant relating $\mathcal{P}_{\rm today}$ and $L_{\rm IR}$ is large, but also that for many purposes, a steady-state approximation of the starburst phenomenon is inadequate, and consequently the functional form relating $\mathcal{P}$ and $L_{\rm IR}$ must be time-dependent. In particular, there is evidence for more than one starbursting region in the nearby galaxy M82, with one of these star forming regions active until $\sim$20 Myr ago, but suppressed over the last 10 to 15 Myr [59,60]. The mean age of the active starburst is $\lesssim$15 Myr [59]. NGC 253 has also a complex structure, with the possibility of two or more (a)synchronous starbursting episodes during its lifetime [61]. The central regions of NGC 253 contain a large population of rather young stars formed within the past $\sim$30 Myr [62].

A second source of uncertainty steams from the shock velocity. Parameterized three-dimensional radiative hydrodynamical simulations that follow the emergence and dynamics of starburst's superwinds seem to indicate that superwinds driven by energy injection in a ringlike geometry can produce a fast ($\gtrsim 0.01\,c$) transient flow along the minor axis [63].

APPENDIX B: PHOTODISINTEGRATION TIMESCALE

In this appendix, we estimate the energy loss rate due to UHECR nucleus photodisintegration. We approximate the starburst core as a cylinder of radius $\sim$200 pc and thickness $\sim$80 pc. The spectral energy density for the radiation fields of M82 inside the core is shown in Fig. 1. It can be approximated by a broken power law,

$$n(\varepsilon) = n_0 \begin{cases} (\varepsilon/\varepsilon_0)^{\alpha} & \varepsilon < \varepsilon_0 \\ (\varepsilon/\varepsilon_0)^{\beta} & \text{otherwise} \end{cases}, \tag{B1}$$

where ε is the photon energy, the maximum photon number density is at an energy of $\varepsilon_0 = 11$ meV, and where $n_0 = 10^6$ cm^{-3} eV^{-1}, $\alpha = 1.1$, and $\beta = -1.8$ [52]. The spectrum is normalized so that the total number density of photons is $\int n(\varepsilon) d\varepsilon$. Out in the halo, $|z| \gtrsim 40$ pc, for $\varepsilon \gtrsim 10^{-3}$ eV, the photon density decreases with the square of the distance, i.e., $n_0 = 10^6$ cm^{-3} eV$^{-1}(z/40\,\mathrm{pc})^{-2}$. For $\varepsilon \lesssim 10^{-3}$ eV, the spectral energy density is dominated by the contribution of the cosmic microwave background.

The photodisintegration timescale of a cosmic ray nucleus, with energy $E = \gamma A m_p$ and Lorentz boost γ, propagating through an isotropic photon background with energy ε and spectral energy density $n(\varepsilon)$ is found to be

$$\frac{1}{\tau_{\rm int}} = \frac{c}{2}\int_0^\infty d\varepsilon \frac{n(\varepsilon)}{\gamma^2\varepsilon^2}\int_0^{2\gamma\varepsilon} d\varepsilon' \varepsilon' \sigma(\varepsilon'), \tag{B2}$$

where $\sigma(\varepsilon')$ is the photodisintegration cross section by a photon of energy ε' in the rest frame of the nucleus, and where A is the nucleus baryon number and m_p the mass of the proton [65].

The photodisintegration cross section is approximated by a single pole in the narrow-width approximation,

$$\sigma(\varepsilon') = \pi\sigma_{\rm res}\frac{\Gamma_{\rm res}}{2}\delta(\varepsilon' - \varepsilon'_{\rm res}), \tag{B3}$$

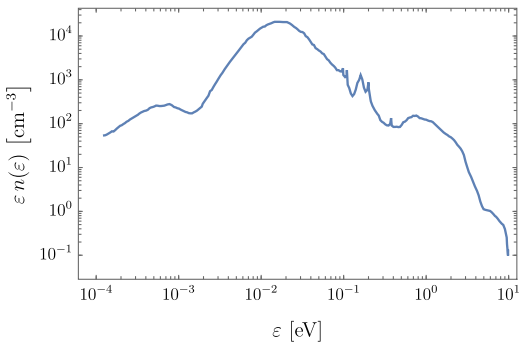

FIG. 1. Spectral energy density for the radiation fields of M82 [64].

where $\sigma_{\rm res} \approx 1.45 \times 10^{-27}$ cm^2 A is the resonance peak, $\Gamma_{\rm res} = 8$ MeV its width, and $\epsilon'_{\rm res} = 42.65 A^{-0.21} \times (0.925 A^{2.433})$ MeV, for $A > 4$ ($A \leq 4$) the pole [66]. The factor of $1/2$ is introduced to match the integral (i.e., total cross section) of the Breit-Wigner and the delta function [67].

Substitution of (B3) into (B2) leads to,

$$\frac{1}{\tau_{\rm int}(E)} \approx \frac{c\pi\sigma_{\rm res}\varepsilon'_{\rm res}\Gamma_{\rm res}}{4\gamma^2}\int_0^\infty \frac{d\varepsilon}{\varepsilon^2} n(\varepsilon)\Theta(2\gamma\varepsilon - \varepsilon'_{\rm res}) = \frac{c\pi\sigma_{\rm res}\varepsilon'_{\rm res}\Gamma_{\rm res}}{4\gamma^2}\int_{\epsilon'_{\rm res}/2\gamma}^\infty \frac{d\varepsilon}{\varepsilon^2} n(\varepsilon). \tag{B4}$$

We adopt the spectral energy density of photons in M82 as benchmark, and so substituting (B1) into (B4) we arrive at

$$\frac{1}{\tau_{\rm int}^{A\gamma}(E)} = \frac{1}{\tau_b}\begin{cases} (E_b/E)^{\beta+1} & E \leq E_b \\ \eta(E) + (E_b/E)^2 & E > E_b \end{cases}, \tag{B5}$$

where

$$\tau_b = \frac{2E_b(1-\beta)}{c\,\pi\,\sigma_{\rm res}\,A\,m_p\,\Gamma_{\rm res}\,n_0}, \tag{B6}$$

$$E_b = \frac{\varepsilon'_{\rm res}\,A\,m_p}{2\varepsilon_0}, \tag{B7}$$

and $\eta(E) = (1-\beta)/(1-\alpha)[(E_b/E)^{\alpha+1} - (E_b/E)^2]$ [68]. A straightforward calculation shows that the photodisintegration timescale of medium mass (carbon, nitrogen, or oxygen) cosmic ray nucleus with $E \gtrsim 10^{10}$ GeV propagating in the photon background at $z \gtrsim 1$ kpc is $\tau_{\rm int}^{A\gamma} \gtrsim 0.1$ Gyr.

Note that for a medium mass nucleus, the energy loss per collision $\sim\gamma m_p$ is negligible when compared to that of baryon scattering. Thus, the energy loss rate of hadronic collisions in the halo is comparable to that of photodisintegration.

In closing, we note that at the peak, the $\Delta(1232)$ resonant cross section is roughly an order of magnitude smaller than the giant-dipole resonance; for ^{16}O, these cross sections peak at 20 MeV and 300 MeV and are roughly 30 mb [69] and 3 mb [70], respectively). Besides, an oxygen nucleus of $10^{10.7}$ GeV has a Lorentz boost $\gamma \sim 10^{9.5}$, and so to excite the $\Delta(1232)$ would require photons with $\varepsilon \sim 0.1$ eV. This is a decade of energy above the peak of the spectrum where the number of photons decreases by more than an order of magnitude, see Fig. 1. Altogether, the interaction timescale of photopion production is orders of magnitude larger than that of photodisintegration.

APPENDIX C: ASSESSING THE NEUTRINO FLUX

High-energy astrophysical neutrinos are the tell-tale signature of hadronic interactions. In this appendix we examine whether the neutrino signal can be used to discriminate acceleration models which take place inside the starburst nuclei from those in which acceleration takes place out in the galactic halo.

Acceleration of UHECRs in the starburst nucleus has been proposed to originate in young neutron star winds [71,72], tidal disruption events [34,73], and llGRB explosions [18]. For relativistic winds of fast-spinning pulsars, the estimated neutrino flux produced while UHECRs cross the supernova ejecta surrounding the stars is within the IceCube reach [74,75].

Independently of the acceleration mechanism, interactions of UHECR within the starburst nucleus could also lead to a measurable neutrino flux. The gas density in the starburst nucleus is related to the star formation rate and hence associated to the IR luminosity via the Kennicutt-Schmidt scaling [76], and is given by

$$n_{{\rm g},n} \sim 100 (L_{\rm IR}/L_{\rm IR,M82})^{0.715}\ {\rm cm}^{-3}, \tag{C1}$$

where, as noted in [51], the exponent of the correlation is in agreement with [77]. Taking the σ_{pA} cross section introduced in Sec. II, it is straightforward to see that the interaction timescale for UHECRs to collide with the background gas is $\mathcal{O}(10^4$ yr). On the other hand, for the radiation background shown in Fig. 1 the photodisintegration timescale in the starburst nucleus is $\mathcal{O}(0.1$ Myr).

In addition, the contribution of nucleus photodisintegration to the neutrino flux originates in the decay of the emitted neutron. Note that the maximum $\bar\nu$ energy in the neutron rest frame is very nearly $Q_{\bar\nu} \equiv m_n - m_p - m_e = 0.78$ MeV, where m_n and m_e are the mass of the neutron and electron, respectively [78]. In the lab, the ratio of the maximum $\bar\nu$ energy to the neutron energy is $Q_{\bar\nu}/m_n \sim 10^{-3}$, and so the boosted $\bar\nu$ has an average energy $E_{\bar\nu} \sim 10^{-3}\gamma m_n$. This is in sharp contrast to baryon scattering, where the maximum neutrino energy could be about 0.1 that of the incoming cosmic ray [79]. Therefore, neutrino production is largely dominated by hadronic collisions on the gas environment of the starburst nucleus. An estimate of the expected diffuse neutrino flux from starbursts assuming UHECR interactions with the gas density given in (C1) has been carried out in [51]. For a neutrino energy in the range $10^6 \lesssim E_\nu/{\rm GeV} \lesssim 10^8$, the estimated single-flavor energy-squared weighted neutrino flux,

$$E_\nu^2 \Phi_\nu \sim 10^{-8.5}\ {\rm GeV\,cm^{-2}\,s^{-1}\,sr^{-1}}, \tag{C2}$$

saturates the IceCube flux/limit [80], and is therefore within reach of next generation experiments.

We have seen in Appendix B that out in the galactic halo, where UHECR accelerated in the starburst superwind could be storaged, the interaction timescale of photodisintegration and/or scattering off the gas is between four to five orders of magnitude larger than the one in the nucleus. Therefore, the associated neutrino flux would be largely suppressed. Indeed the expected neutrino flux would be below the cosmogenic neutrino flux and out of reach of next generation experiments; see Fig. 9 in [51].

[1] J. Linsley, Evidence for a Primary Cosmic-Ray Particle with Energy 10^{20} eV, Phys. Rev. Lett. **10**, 146 (1963).
[2] L. A. Anchordoqui, Ultra-high-energy cosmic rays, Phys. Rep. **801**, 1 (2019).
[3] L. A. Anchordoqui, G. E. Romero, and J. A. Combi, Heavy nuclei at the end of the cosmic ray spectrum?, Phys. Rev. D **60**, 103001 (1999).
[4] L. A. Anchordoqui, H. Goldberg, and D. F. Torres, Anisotropy at the end of the cosmic ray spectrum?, Phys. Rev. D **67**, 123006 (2003).
[5] J. Abraham *et al.* (Pierre Auger Collaboration), Measurement of the Depth of Maximum of Extensive Air Showers Above 10^{18} eV, Phys. Rev. Lett. **104**, 091101 (2010).
[6] A. Aab *et al.* (Pierre Auger Collaboration), Depth of maximum of air-shower profiles at the Pierre Auger Observatory: Measurements at energies above $10^{17.8}$ eV, Phys. Rev. D **90**, 122005 (2014).
[7] A. Aab *et al.* (Pierre Auger Collaboration), Depth of maximum of air-shower profiles at the Pierre Auger Observatory II: Composition implications, Phys. Rev. D **90**, 122006 (2014).
[8] A. Aab *et al.* (Pierre Auger Collaboration), Evidence for a mixed mass composition at the 'ankle' in the cosmic-ray spectrum, Phys. Lett. B **762**, 288 (2016).
[9] A. Aab *et al.* (Pierre Auger Collaboration), Inferences on mass composition and tests of hadronic interactions from 0.3 to 100 EeV using the water-Cherenkov detectors of the Pierre Auger Observatory, Phys. Rev. D **96**, 122003 (2017).
[10] A. A. Watson, Further evidence for an increase of the mean mass of the highest-energy cosmic-rays with energy, J. High Energy Astrophys. **33**, 14 (2022).
[11] A. Aab *et al.* (Pierre Auger Collaboration), An indication of anisotropy in arrival directions of ultra-high-energy cosmic rays through comparison to the flux pattern of extragalactic gamma-ray sources, Astrophys. J. Lett. **853**, L29 (2018).
[12] P. Abreu *et al.* (Pierre Auger Collaboration), Arrival directions of cosmic rays above 32 EeV from phase one of the Pierre Auger Observatory, Astrophys. J. **935**, 170 (2022).
[13] A. di Matteo *et al.* (Pierre Auger and Telescope Array Collaborations), 2022 report from the Auger-TA working group on UHECR arrival directions, arXiv:2302.04502.
[14] R. Higuchi, T. Sako, T. Fujii, K. Kawata, and E. Kido, Effects of galactic magnetic field on the UHECR correlation studies with starburst galaxies, arXiv:2209.00305.
[15] IceCube, Pierre Auger, and Telescope Array Collaborations, Search for correlations between the arrival directions of IceCube neutrino events and ultrahigh-energy cosmic rays detected by the Pierre Auger Observatory and the Telescope Array, J. Cosmol. Astropart. Phys. 01 (2016) 037.
[16] T. M. Heckman and T. A. Thompson, A brief review of galactic winds, arXiv:1701.09062.
[17] R. Alves Batista, J. Biteau, M. Bustamante, K. Dolag, R. Engel, K. Fang, K. H. Kampert, D. Kostunin, M. Mostafa, K. Murase *et al.*, Open questions in cosmic-ray research at ultrahigh energies, Front. Astron. Space Sci. **6**, 23 (2019).
[18] B. T. Zhang, K. Murase, S. S. Kimura, S. Horiuchi, and P. Mészáros, Low-luminosity gamma-ray bursts as the sources of ultrahigh-energy cosmic ray nuclei, Phys. Rev. D **97**, 083010 (2018).
[19] N. Bergvall, T. Marquart, M. J. Way, A. Blomqvist, E. Holst, G. Östlin, and E. Zackrisson, Local starburst galaxies and their descendants, Astron. Astrophys. **587**, A72 (2016).
[20] J. S. Ulvestad and R. R. J. Antonucci, Do the compact radio sources in NGC 253 and M82 fade over time?, Astrophys. J. **424**, L32 (1994).
[21] P. M. Dragicevich, D. G. Blair, and R. R. Burman, Why are supernovae in our Galaxy so frequent?, Mon. Not. R. Astron. Soc. **302**, 693 (1999).
[22] L. A. Anchordoqui, C. Mechmann, and J. F. Soriano, Toward a robust inference method for the likelihood of low-luminosity gamma-ray bursts to be progenitors of ultrahigh-energy cosmic rays correlating with starburst galaxies, J. High Energy Astrophys. **25**, 23 (2020).
[23] L. A. Anchordoqui, Acceleration of ultrahigh-energy cosmic rays in starburst superwinds, Phys. Rev. D **97**, 063010 (2018).
[24] L. A. Anchordoqui and D. F. Torres, Exploring the superwind mechanism for generating ultrahigh-energy cosmic rays using large-scale modeling of starbursts, Phys. Rev. D **102**, 023034 (2020).
[25] A. M. Hillas, The origin of ultrahigh-energy cosmic rays, Annu. Rev. Astron. Astrophys. **22**, 425 (1984).
[26] E. Waxman, Cosmological Gamma-Ray Bursts and the Highest Energy Cosmic Rays, Phys. Rev. Lett. **75**, 386 (1995).
[27] J. H. Matthews, A. R. Bell, K. M. Blundell, and A. T. Araudo, Fornax A, Centaurus A, and other radio galaxies as sources of ultrahigh energy cosmic rays, Mon. Not. R. Astron. Soc. **479**, L76 (2018).
[28] T. M. Heckman, L. Armus, and G. K. Miley, On the nature and implications of starburst-driven galactic superwinds, Astrophys. J. Suppl. Ser. **74**, 833 (1990).
[29] J. D. Bregman, P. Temi, and D. Rank, Direct measurement of the supernova rate in starburst galaxies, Astron. Astrophys. **355**, 525 (2000).

[30] D. B. Sanders, J. M. Mazzarella, D. C. Kim, J. A. Surace, and B. T. Soifer, The IRAS revised bright galaxy sample (RBGS), Astron. J. **126**, 1607 (2003).
[31] E. Fermi, Galactic magnetic fields and the origin of cosmic radiation, Astrophys. J. **119**, 1 (1954).
[32] H. Engel, R. I. Davies, R. Genzel, L. J. Tacconi, E. Sturm, and D. Downes, Arp220: Extinction and merger-induced star formation, Astrophys. J. **729**, 58 (2011).
[33] R. Parra, J. E. Conway, P. J. Diamond, H. Thrall, C. J. Lonsdale, C. J. Lonsdale, and H. E. Smith, The radio spectra of the compact sources in Arp 220: A mixed population of supernovae and supernova remnants, Astrophys. J. **659**, 314 (2007).
[34] D. N. Pfeffer, E. D. Kovetz, and M. Kamionkowski, Ultrahigh-energy cosmic ray hotspots from tidal disruption events, Mon. Not. R. Astron. Soc. **466**, 2922 (2017).
[35] G. E. Romero, A. L. Müller, and M. Roth, Particle acceleration in the superwinds of starburst galaxies, Astron. Astrophys. **616**, A57 (2018).
[36] K. Tomisaka and J. N. Bregman, Extended hot gas halos around starburst galaxies, Publ. Astron. Soc. Jpn. **45**, 513 (1993).
[37] D. K. Strickland and I. R. Stevens, Starburst-driven galactic winds: I. energetics and intrinsic x-ray emission, Mon. Not. R. Astron. Soc. **314**, 511 (2000).
[38] M. Sharma, B. B. Nath, I. Chattopadhyay, and Y. Shchekinov, Interaction of a galactic wind with halo gas and the origin of multiphase extraplanar material, Mon. Not. R. Astron. Soc. **441**, 431 (2014).
[39] B. Abu-Ibrahim and A. Kohama, Scaling properties of proton-nucleus total reaction cross sections, Phys. Rev. C **81**, 057601 (2010).
[40] I. L. Rasmussen and B. Peters, The nuclear composition of cosmic rays at their source in a closed galaxy, Nature (London) **258**, 412 (1975).
[41] B. J. Buckman, T. Linden, and T. A. Thompson, Cosmic rays and magnetic fields in the core and halo of the starburst M82: Implications for galactic wind physics, Mon. Not. R. Astron. Soc. **494**, 2679 (2020).
[42] D. G. Wentzel, Cosmic-ray propagation in the galaxy: Collective effects, Annu. Rev. Astron. Astrophys. **12**, 71 (1974).
[43] P. Blasi and A. V. Olinto, A magnetized local supercluster and the origin of the highest energy cosmic rays, Phys. Rev. D **59**, 023001 (1999).
[44] T. K. Gaisser, *Cosmic Rays and Particle Physics* (Cambridge University Press, Cambridge, England, 1990), ISBN 0-521-33931-6.
[45] D. K. Strickland, Starburst-driven galactic superwinds, ASP Conf. Ser. **253**, 387 (2002).
[46] C. F. Jones, J. H. Crawford, J. Engelage, G. T. Guzik, W. J. Mitchell, J. C. Waddington, R. W. Webber, and P. J. Wefel, The leaky box: An idea whose time is up?, in *Proceedings of the 21st International Cosmic Ray Conference* (1990), Vol. 3, p. 333.
[47] I. D. Karachentsev, V. E. Karachentseva, W. K. Huchtmeier, and D. I. Makarov, A catalog of neighboring galaxies, Astron. J. **127**, 2031 (2004).
[48] T. Oosterloo, F. Fraternali, and R. Sancisi, The cold gaseous halo of NGC 891, Astron. J. **134**, 1019 (2007).
[49] R. Temple, S. Raychaudhury, and I. Stevens, X-ray observations of the edge-on star-forming galaxy NGC 891 and its supernova SN1986J, Mon. Not. R. Astron. Soc. **362**, 581 (2005).
[50] R. U. Abbasi *et al.* (Telescope Array Collaboration), Indications of a cosmic ray source in the Perseus-Pisces supercluster, arXiv:2110.14827.
[51] A. Condorelli, D. Boncioli, E. Peretti, and S. Petrera, Testing hadronic and photo-hadronic interactions as responsible for UHECR and neutrino fluxes from Starburst Galaxies, Phys. Rev. D **107**, 083009 (2023).
[52] M. S. Muzio and G. R. Farrar, Constraints on the hosts of UHECR accelerators, Astrophys. J. Lett. **942**, L39 (2023).
[53] C. Leitherer, D. Schaerer, J. D. Goldader, R. M. Gonzalez Delgado, C. Robert, D. F. Kune, D. F. d. Mello, D. Devost, and T. M. Heckman, Starburst99: Synthesis models for galaxies with active star formation, Astrophys. J. Suppl. Ser. **123**, 3 (1999).
[54] E. E. Salpeter, The luminosity function and stellar evolution, Astrophys. J. **121**, 161 (1955).
[55] S. Veilleux, G. Cecil, and J. Bland-Hawthorn, Galactic winds, Annu. Rev. Astron. Astrophys. **43**, 769 (2005).
[56] D. A. Hunter, F. C. Gillet, J. S. Gallagher III, W. L. Rice, and F. J. Low, IRAS observations of a small sample of blue irregular galaxies, Astrophys. J. **303**, 171 (1986).
[57] C. Leitherer, The upper initial mass function in starburst galaxies, ASP Conf. Ser. **142**, 61 (1998).
[58] R. A. W. Elson, S. M. Fall, and K. C. Freeman, The stellar content of rich young clusters in the large magellanic cloud, Astrophys. J. **336**, 734 (1989).
[59] R. de Grijs, R. W. O'Connell, and J. S. Gallagher III, The fossil starburst in M82, Astron. J. **121**, 768 (2001).
[60] R. de Grijs, Star formation time-scales in the nearby, prototype starburst galaxy M82, Astron. Geophys. **42**, 12 (2001).
[61] T. J. Davidge, Shaken, not stirred: The disrupted disk of the starburst galaxy NGC 253, Astrophys. J. **725**, 1342 (2010).
[62] T. J. Davidge, The compact star-forming complex at the heart of NGC 253, Astrophys. J. **818**, 142 (2016).
[63] D. D. Nguyen and T. A. Thompson, Galactic winds and bubbles from nuclear starburst rings, Astrophys. J. Lett. **935**, L24 (2022).
[64] B. C. Lacki and T. A. Thompson, Diffuse hard X-ray emission in starburst galaxies as synchrotron from very high energy electrons, Astrophys. J. **762**, 29 (2013).
[65] F. W. Stecker, Photodisintegration of ultrahigh-energy cosmic rays by the universal radiation field, Phys. Rev. **180**, 1264 (1969).
[66] S. Karakula and W. Tkaczyk, The formation of the cosmic ray energy spectrum by a photon field, Astropart. Phys. **1**, 229 (1993).
[67] L. A. Anchordoqui, J. F. Beacom, H. Goldberg, S. Palomares-Ruiz, and T. J. Weiler, TeV γ^- rays and neutrinos from photo-disintegration of nuclei in Cygnus OB2, Phys. Rev. D **75**, 063001 (2007).
[68] M. Unger, G. R. Farrar, and L. A. Anchordoqui, Origin of the ankle in the ultrahigh energy cosmic ray spectrum, and of the extragalactic protons below it, Phys. Rev. D **92**, 123001 (2015).

[69] N. Lyutorovich, V. I. Tselyaev, J. Speth, S. Krewald, F. Grummer, and P. G. Reinhard, Self-Consistent Calculations of the Electric Giant Dipole Resonances in Light and Heavy Mass Nuclei, Phys. Rev. Lett. **109**, 092502 (2012).
[70] L. Morejon, A. Fedynitch, D. Boncioli, D. Biehl, and W. Winter, Improved photomeson model for interactions of cosmic ray nuclei, J. Cosmol. Astropart. Phys. 11 (2019) 007.
[71] P. Blasi, R. I. Epstein, and A. V. Olinto, Ultrahigh-energy cosmic rays from young neutron star winds, Astrophys. J. Lett. **533**, L123 (2000).
[72] L. A. Anchordoqui, V. Barger, and T. J. Weiler, Cosmic mass spectrometer, J. High Energy Astrophys. **17**, 38 (2018).
[73] G. R. Farrar and T. Piran, Tidal disruption jets as the source of ultra-high energy cosmic rays, arXiv:1411.0704.
[74] K. Fang, K. Kotera, K. Murase, and A. V. Olinto, Testing the newborn pulsar origin of ultrahigh energy cosmic rays with EeV neutrinos, Phys. Rev. D **90**, 103005 (2014); **92**, 129901 (E) (2015).
[75] K. Fang, K. Kotera, K. Murase, and A. V. Olinto, IceCube constraints on fast-spinning pulsars as high-energy neutrino sources, J. Cosmol. Astropart. Phys. 04 (2016) 010.
[76] R. C. Kennicutt, Jr., The global Schmidt law in star forming galaxies, Astrophys. J. **498**, 541 (1998).
[77] R. C. Kennicutt, Jr. and N. J. Evans II, Star formation in the Milky Way and nearby galaxies, Annu. Rev. Astron. Astrophys. **50**, 531 (2012).
[78] L. A. Anchordoqui, H. Goldberg, F. Halzen, and T. J. Weiler, Galactic point sources of TeV antineutrinos, Phys. Lett. B **593**, 42 (2004).
[79] M. Ahlers, L. A. Anchordoqui, H. Goldberg, F. Halzen, A. Ringwald, and T. J. Weiler, Neutrinos as a diagnostic of cosmic ray galactic/extra-galactic transition, Phys. Rev. D **72**, 023001 (2005).
[80] R. Abbasi *et al.* (IceCube Collaboration), The IceCube high-energy starting event sample: Description and flux characterization with 7.5 years of data, Phys. Rev. D **104**, 022002 (2021).